MATHEMATICAL ANALYSIS, MODELING AND OPTIMIZATION OF COMPLEX HEAT TRANSFER PROCESSES

Dr. Uldis Raitums, Dr. Kārlis Birģelis

Goals of research

To develop and investigate mathematical properties of algorithms for numerical optimization of heat transfer processes in nonlinear systems with nonlocal boundary conditions.

Planned tasks and activities

The main research activities in this project we have planned to focus on investigation of special class of optimal control problems, applied to optimize complex physical systems, where heat transfer occurs simultaneously in different ways – due to heat conduction, convection and heat radiation propagation, Typically, problems of this class consist of two parts:

1. A nonlinear system of partial differential and integral equations, which describes dependence of temperature field as state variable from other control parameters;
2. A cost functional, against which optimization is carried out.

All research activities we plan to divide into two different stages:

1. At first stage we planned to make all necessary theoretical analysis of the problem in order to obtain auxiliary results, which could be used at second stage of research activities (for example, finding of an algorithm how to construct a minimizing sequence of controls, or finding of a formula for calculation of the gradient of the cost functional). As it is expected, obtaining of these theoretical results will not be easy due to nonlinear and nonlocal dependence of the state and control parameters in the state equation.
2. At second stage we planned to develop numerical methods and apply them for simple test problems. As it is expected, that here we will not be able to use standard numerical methods, but we will need to develop special methods used only for this case.

1.Problem formulation

To optimize heat transfer processes in complicated physical systems, where various physical phenomena simultaneously occur – heat conduction and convection, heat radiation propagation, we can use standard optimization techniques.
Typically, mathematical formalization for the given class of problems leads to the following type of optimal control problems:

$$\begin{cases} J(v,u) \longrightarrow min, \\ A(v,u) = 0, \\ u \in U. \end{cases} \quad (1)$$

Here v denotes a state parameter, u – a control parameter, U – a set of admissible controls, $J(v,u)$ - a cost functional, which "measures" optimality of a freely chosen

parameter pair (u, v), but $A(v, u) = 0$ - a state equation, which defines relationship between state and control parameters.

In order to investigate mathematical properties and derive numerical methods for solving of the given class of problems about modeling and optimization of complicated heat transfer processes in physical systems, we chose as model a real world problem from glass fabric industry about temperature field optimization in high temperature furnaces (see paper of A.Buikis and A.D.Fitt [5]).

Let the furnace has the following design - it consists of simple cylindrical heater wrapped around constantly moving glass fabric sheet (see Fig. 1). Let $\Omega_1 = (0, l_1) \times (-l_2, l_2) \times (-l_3, l_3)$ is a part of the fabric lying directly inside the furnace. The inflow boundary $\{0\} \times (-l_2, l_2) \times (-l_3, l_3)$ we denote by Γ_1 and outflow boundary $\{l_1\} \times (-l_2, l_2) \times (-l_3, l_3)$ by Γ_2. A volume of air surrounding both fabric and heater let us denote by Ω_2. The boundary $\partial\Omega_2$ of this domain splits into three disjoint parts Σ_1, Σ_2, Σ_3, where Σ_1 is fabric-air interface, Σ_2 is heater-air interface and Σ_3 ir remainder of the domain boundary $\partial\Omega_2$ (marked with dotted line in Fig. 1).

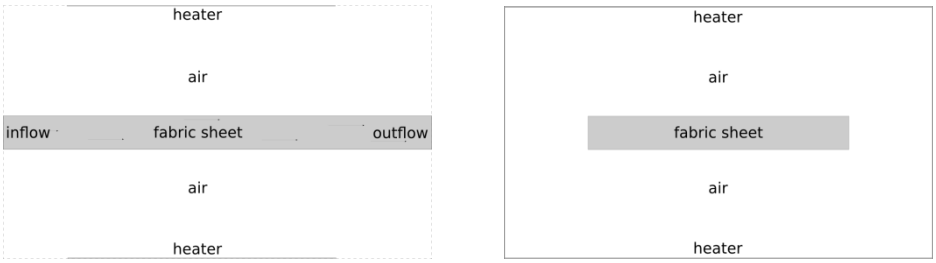

x_1, x_3 cross section x_2, x_3 cross section

Figure 1. Geometry of the furnace.

Let n_1, n_2 denotes outward normal to Ω_1, Ω_2, respectively. Let us also denote the sets: $\Lambda := \Omega_2 \times S$, $\Lambda^+ := \partial\Omega_2 \times \{\omega \in S : \omega \cdot n_2 \geq 0\}$, $\Lambda^- := \partial\Omega_2 \times \{\omega \in S : \omega \cdot n_2 < 0\}$, where $S = \{\omega \in \mathbb{R}^3 : |\omega| = 1\}$ is unit sphere. If v is a function defined on $\Omega \times S$, where Ω is some domain, then by $(\nabla, \omega)v$ we denote directional derivative of this function in the direction ω.

Due to different physical characteristics of air and fabric there will be very different heat transfer processes in each of the components of multi-domain system Ω_1, Ω_2. Since fabric is almost opaque for heat radiation, then heat conduction and convection (due to fabric drift) will prevail over other heat transfer forms in Ω_1. At the same time, since air is transparent for heat radiation and working temperature of furnace is high enough (about 1100K) to produce significant radiative heat flux through air-solid interface then radiative heat transfer will dominate over other heat processes in Ω_2.

Since heat conduction and convection prevail in Ω_1 then for temperature field $T_f(x)$ in this domain we will have the following equation:

$$k_1 \Delta T_f - k_2 \frac{\partial T_f}{\partial x_1} = 0 \quad \text{on } \Omega_1 \tag{2}$$

To describe radiative heat transfer in Ω_2 we can use models proposed in [2], [8]. If we assume that Ω_2 is filled with transparent and nonparticipating medium and $\partial\Omega_2$ emits, absorbs and reflects heat radiation like gray surface, then at thermal equilibrium for heat radiation intensity $I(x, \omega)$ (measures photon flux intensity at point x traveling into direction ω) in $\Omega_2 \times S$ and it traces $I^+(x, \omega)$, $I^-(x, \omega)$ on the sets Λ^+, Λ^-, respectively, we will have the following system:

$$(\nabla, \omega) I = 0 \quad \text{in } \Lambda \tag{3}$$

and

$$I^-(x,\omega) = \frac{\epsilon\sigma T^4}{\pi} + \frac{(1-\epsilon)}{\pi}\int_{n_2\cdot\omega'\geq 0} I^+(x,\omega')(n_2\cdot\omega')d\omega' \quad \text{on } \Lambda^-, \tag{4}$$

where $\varepsilon(x)$ and $T(x)$ are emissivity and temperature fields on $\partial\Omega_2$ defined as

$$\varepsilon(x) := \begin{cases} \varepsilon_f & \text{on } \Sigma_1, \\ \varepsilon_h & \text{on } \Sigma_2, \\ 1 & \text{on } \Sigma_3, \end{cases} \qquad T(x) := \begin{cases} T_f(x) & \text{on } \Sigma_1, \\ T_h(x) & \text{on } \Sigma_2, \\ 0 & \text{on } \Sigma_3. \end{cases}$$

For total heat flux on the fabric-air interface Σ_1 we will have the following equation

$$-k_1\frac{\partial T_f}{\partial n_1} = \varepsilon\sigma T_f^4 - \varepsilon\int_{n_2\cdot\omega'\geq 0} I^+(x,\omega')(n_2\cdot\omega')d\omega' + k_3\left(T_f - T_g\right). \tag{5}$$

The first two terms in right hand side of this equation describe radiative part of total flux through Σ_1, whereas the last term describes heat flux determined by Newton type heat exchange between fabric and air (having fixed temperature $T_g(x)$ on Σ_1). In addition, let us assume that

$$\begin{cases} T_f = T_e & \text{on } \Gamma_1, \\ -k_1\frac{\partial T_f}{\partial n_1} = 0 & \text{on } \Gamma_2, \end{cases} \tag{6}$$

for some fixed T_e as element of $W_2^1(\Omega_1)$.

To fulfill a task and optimize steady state temperature field of the fabric sheet $T_f(x)$, we choose some target temperature profile $T_t(x)$ on Ω_1 and define a cost functional

$$J(T_f, T_h) := \int_{\Omega_1}\left(T_f - T_t\right)^2 dx + \frac{\alpha}{2}\int_{\Sigma_2} T_h^2 ds, \tag{7}$$

where $\alpha \in (0, +\infty)$ is some regularization parameter (usually it has value in range from 10^{-5} to 10^{-6}). Minimization of this functional is equivalent to force real temperature T_f be as close as possible to the profile T_t. At the same time we must take into account that T_f is determined by (2), (3), (4), (5), (6). Actually, these equations show how T_f depends from other characteristics of the furnace - heater temperature, geometry of furnace, velocity of fabric drift, etc. We can use these characteristics to control T_f while minimizing (7).

If we choose heater temperature $T_h(x)$ as control parameter, then optimization problem for making T_f as close as possible to T_t reads as

$$\begin{cases} J(T_f, T_h) = \int_{\Omega_1}\left(T_f - T_t\right)^2 dx + \frac{\alpha}{2}\int_{\Sigma_2} T_h^2 ds \longrightarrow min, \\ \text{subject to } (2), (3), (4), (5), (6), \\ T_h \in U, \end{cases} \tag{8}$$

where the set of admissible controls is defined as

$$U := \{v \in L_\infty(\Sigma_2) : \ \mu_1 \leq v(x) \leq \mu_2\}$$

for some fixed $\mu_1 \in (0, +\infty)$, $\mu_2 \in [\mu_1, +\infty)$.

2. Theoretical results

Before we present some theoretical results, let us start by introducing some general definitions.

DEFINITIONS

First of all, the standard Lebesgue and Sobolev spaces let us denote by $L_p(A)$ (A is an arbitrary set equipped with some measure and $p \in [1, +\infty]$) and $W_2^1(\Omega)$ (Ω is an arbitrary bounded Lipschitz domain in $\mathbb{R}^3$). In addition, let us introduce the following functional spaces:

- $W_2^1(\Omega, \Gamma) := \{v \in W_2^1(\Omega) : v|_\Gamma = 0 \ \text{ a. e. on } \Gamma\}$, where $\Gamma \subset \partial\Omega$;

- $V_5(\Omega,\Gamma) := \{v \in W_2^1(\Omega) : v|_\Gamma \in L_5(\Gamma)\}$, where $\Gamma \subset \partial\Omega$. The norm here we define by $\|v\|_{V_5(\Omega,\Gamma)} = \|v\|_{W_2^1(\Omega)} + \|v\|_{L_5(\Gamma)}$;
- $\dot{V}_5(\Omega,\Gamma_1,\Gamma_2) := \{v \in W_2^1(\Omega,\Gamma_1) : v|_{\Gamma_2} \in L_5(\Gamma_2)\}$, where $\Gamma_1,\Gamma_2 \subset \partial\Omega$. The norm here we define by $\|v\|_{\dot{V}_5(\Omega,\Gamma_1,\Gamma_2)} = \|v\|_{W_2^1(\Omega,\Gamma_1)} + \|v\|_{L_5(\Gamma_2)}$;
- $H_{5/4}(\Omega \times S)$ is a Banach space consisting of all functions $v: \Omega \times S \to \mathbb{R}$, which together with their directional derivatives (in the sense of distributions) $(\nabla,\omega)v$ belong to $L_{5/4}(\Omega \times S)$. In context of this space we will also consider the weighted Lebesgue spaces $\tilde{L}_{5/4}(A)$ (A is an arbitrary measurable subset of $\partial\Omega \times S$), where traces of the functions $v \in H_{5/4}(\Omega \times S)$ belong (see [2]);

By $\boldsymbol{E}$ we denote identity operator mapping appropriate functional spaces into itself. By W^* we denote dual space of an arbitrary Banach space W and by $\langle f, v\rangle_W$ - duality pairing between elements $f \in W^*$, $v \in W$.

Throughout this paper we will put the following restrictions on geometry of the furnace:

A1 $\Omega_1 := (0,l_1) \times (-l_2,l_2) \times (-l_3,l_3)$, where $l_1 \in (0,+\infty)$, $l_2 \in (0,+\infty)$, $l_3 \in (0,+\infty)$;

A2 Ω_2 is bounded Lipschitz domain;

A3 $\partial\Omega_1 \cap \partial\Omega_2 = \partial\Omega_1 \setminus (\Gamma_1 \cup \Gamma_2)$, where $\Gamma_1 := \{0\} \times (-l_2,l_2) \times (-l_3,l_3)$ and $\Gamma_2 := \{l_1\} \times (-l_2,l_2) \times (-l_3,l_3)$.

Let us also suppose that the following hypotheses hold for variables and constants found in (8):

B1 $k_1 \in (0,+\infty)$, $k_2 \in (0,+\infty)$, $k_3 \in (0,+\infty)$, $\sigma \in (0,+\infty)$, $\varepsilon_f \in (0,1]$, $\varepsilon_h \in (0,1]$;

B2 $T_e \in V_5(\Omega_1,\Sigma_1)$, $T_t \in L_2(\Omega_1)$, $T_h \in L_\infty(\Sigma_2)$, $T_g \in L_\infty(\Sigma_1)$ and there exist some $\mu_1 \in (0,+\infty)$, $\mu_2 \in [\mu_1,+\infty)$ such that:

$$\mu_1 \le T_e(x) \le \mu_2 \quad \text{a. e on } \Gamma_1;$$
$$\mu_1 \le T_g(x) \le \mu_2 \quad \text{a. e on } \Sigma_1;$$
$$\mu_1 \le T_h(x) \le \mu_2 \quad \text{a. e on } \Sigma_2.$$

Let us also define:

$$X := \{v : v = w + T_e, w \in \dot{V}_5(\Omega_1,\Gamma_1,\Sigma_1)\} \times H_{5/4}(\Lambda).$$

CONTROL-TO-STATE OPERATOR

Using already developed techniques (see also [3], [4], or [8]) the following result can be proved about existence of control-to-state operator:

Theorem 1 [Existence of control-to-state operator].

Under hypotheses A1-A3, B1-B2 for every fixed control $T_h \in U$ there exists one and only one feasible state $(T_f, I) \in X$ of (8)*, i.e. there exists unique defined control-to-state operator*

$$\boldsymbol{\Phi}(T_h) = \begin{pmatrix} \boldsymbol{\Phi_1}(T_h) \\ \boldsymbol{\Phi_2}(T_h) \end{pmatrix}$$

of (8) *as mappings from U to $W_2^1(\Omega_1) \times H_{5/4}(\Lambda)$.*

The following result about boundedness of the state T_f is important for further analysis:

Theorem 2 [Boundedness of state].

Under hypotheses A1-A3, B1-B2 for every fixed control $T_h \in U$ the following estimate holds:

$$\mu_1 \le \boldsymbol{\Phi_1}(T_h) \le \mu_2 \quad \text{a. e on } \Omega_1.$$

Now, if we exclude the variables I, I^+, I^- from the state equation of (8) and take into account the previous result about boundedness of T_f, then the state equation can be rewritten in a weak form:

$$\int_{\Omega_1}\left(k_1(\nabla T_f\cdot\nabla\eta)+k_2\frac{\partial T_f}{\partial x_1}\eta\right)dx+\int_{\Sigma_1}k_3(T_f-T_g)\eta ds +\sigma\int_{\Sigma_1}\left[(\boldsymbol{E}-\boldsymbol{H_1})\left(\psi(T_f)\right)-\boldsymbol{H_2}(\psi(T_h))\right]\eta ds \quad \forall\eta\in \dot{V}_5(\Omega_1,\Gamma_1,\Sigma_1), \qquad (9)$$

where $T_f\in\{v: v=w+T_e, w\in\dot{V}_5(\Omega_1,\Gamma_1,\Sigma_1)\}$ is unknown parameter, $\boldsymbol{H_1}\in\mathcal{L}\left(L_{5/4}(\Sigma_1)\to L_{5/4}(\Sigma_1)\right)$ and $\boldsymbol{H_2}\in\mathcal{L}\left(L_{5/4}(\Sigma_2)\to L_{5/4}(\Sigma_1)\right)$ are nonlocal operators, but function $\psi:\mathbb{R}\to\mathbb{R}$ is defined in such a way that at interval $[0,\mu_2]$ it coincide with the mapping $t\to t^4$, but at infinity it has linear growth rate:

$$\psi(t):=\begin{cases}|t|^3t & |t|\le\mu_2,\\ 4\mu_2^3t-3\mu_2^4 & t>\mu_2,\\ 4\mu_2^3t+3\mu_2^4 & -t>\mu_2.\end{cases}$$

2.1.Gradient formula

In order to apply suitable numerical methods for solving of optimal control problems, it is important to know mathematical properties of a cost functional. For example, if we apply gradient or gradient projection type methods for solving of optimal control problems, it is important to know basic smoothness properties of the cost functional and a way how to calculate gradient of a cost functional.

We have the following result about differentiability of the cost functional $J(\boldsymbol{\Phi_1}(T_h),T_h)$ of (8):

Theorem 3 [Differentiability of cost functional].

If the hypotheses A1-A3, B1-B2 hold, then for every two arbitrary chosen controls $T_h\in U$, $T_h+\delta T_h\in U$ the following formula holds:

$$J(\boldsymbol{\Phi_1}(T_h+\delta T_h),T_h+\delta T_h) = J(\boldsymbol{\Phi_1}(T_h),T_h)+\int_{\Sigma_2}l[T_h]\delta T_h ds+o[T_h]\left(\|\delta T_h\|_{L_\infty(\Sigma_2)}\right),$$

where the derivative $l[T_h]\in L_1(\Sigma_2)$ has the representation

$$l[T_h]=-4\varepsilon_h|T_h|^3\left(\int_{n_2\cdot\omega'\ge0}I_*^+(x,\omega')(n_2\cdot\omega')d\omega'\right)+\alpha T_h \qquad (11)$$

and $(\vartheta_*,I_*)\in W_2^1(\Omega_1,\Gamma_1)\times H_{5/4}(\Lambda)$ is the solution of the adjoint problem:

$$\begin{cases} k_1\Delta\vartheta_*-k_2\frac{\partial\vartheta_*}{\partial x_1}=2(T_f-T_t) & \text{in } \Omega_1,\\ -k_1\frac{\partial\vartheta_*}{\partial n_1}=4\left|T_f\right|^3\varepsilon_f\left(\sigma\vartheta_*-\int_{n_2\cdot\omega'\ge0}I_*^+(x,\omega')(n_2\cdot\omega')d\omega'\right)+k_3\vartheta_* & \text{on } \Sigma_1,\\ -k_1\frac{\partial\vartheta_*}{\partial n_1}=k_2\vartheta_* & \text{on } \Gamma_2,\\ (\nabla,\omega)I_*=0 & \text{on } \Lambda,\\ I_*^-(x,\omega)=\frac{\epsilon\sigma w_*}{\pi}+\frac{(1-\epsilon)}{\pi}\int_{n_2\cdot\omega'\ge0}I_*^+(x,\omega')(n_2\cdot\omega')d\omega' & \text{on } \Lambda^-, \end{cases} \qquad (12)$$

where

$$w_*=\begin{cases}\vartheta_* & \text{on } \Sigma_1,\\ 0 & \text{on } \Sigma_2,\\ 0 & \text{on } \Sigma_3.\end{cases}$$

Similarly as it was done in case of the state equation, we can also rewrite the adjoint problem (12) in a weak form. If we exclude the variables I_*, I_*^+, I_*^- from the ajoint equation, then we will obtain:

$$\int_{\Omega_1}\left(k_1(\nabla\vartheta_*\cdot\nabla\eta)-k_2\frac{\partial\vartheta_*}{\partial x_1}\eta\right)dx+\int_{\Gamma_2}k_2\vartheta_*\eta ds$$
$$+\int_{\Sigma_1}k_3\vartheta_*\eta ds+\sigma\int_{\Sigma_1}\psi'(T_f)[(\boldsymbol{E}-\boldsymbol{H_1})(\vartheta_*)]\eta ds$$
$$=-\int_{\Omega_1}2(T_f-T_t)\eta dx \quad \forall\eta\in W_2^1(\Omega_1,\Gamma_1), \tag{13}$$

where $\vartheta_*\in W_2^1(\Omega_1,\Gamma_1)$ is unknown variable.

3. Optimization algorithms

We are using gradient projection type method for numerical optimization of the problem (8).

1.1.Gradient projection method

Gradient and gradient projection type methods are widely used in numerical optimization due to simplicity and relatively high efficiency of these methods.

However, if we want successfully to apply such type of optimization methods, then cost functional of the optimization problem must have some smoothness properties. In addition, we must also have formula, using which to calculate gradient of the cost functional.

In case of the problem (8) for gradient calculation of the cost functional $J(\boldsymbol{\Phi_1}(T_h),T_h)$ we can use the formula (11). As it turns out, this formula allows us to calculate gradient of the cost functional effectively and with great precision. If we, for example, compare this with numerical differentiation, then the formula (11) is much superior in terms of precision and usage of computation resources. If we would use numerical differentiation, then every gradient calculation requires numerous times of solving of the state equation. At the same time, if we would use the formula (11), then every gradient calculation requires only one time of solving of the state equation and one time of solving of the adjoint problem (12).

To generate minimizing sequence of control parameters starting from some initial guess $T_{h0}\in U$, we are using the following gradient projection algorithm:

$$\begin{cases} T_h^{(i+1)}=\min\left\{\max\left\{T_h^{(i)}-\alpha^{(i)}l\left[T_h^{(i)}\right],\mu_1\right\},\mu_2\right\} \quad i=1,2,\dots,\\ T_h^{(0)}=T_{h0}. \end{cases} \tag{14}$$

Here coefficients $\alpha^{(i)}\in[0,+\infty)$ are usually calculated using some line search algorithm. To guarantee that

$$J\left(\boldsymbol{\Phi_1}\left(T_h^{(i+1)}\right),T_h^{(i+1)}\right)\le J\left(\boldsymbol{\Phi_1}\left(T_h^{(i)}\right),T_h^{(i)}\right) \quad i=1,2,\dots$$

we defined $\alpha^{(i)}:=\max\{A^{(i)}\}$, where

$$A^{(i)}=\{\gamma\beta^j : j=1,2,\dots,$$
$$J(\boldsymbol{\Phi_1}(T_h^*),T_h^*)<J\left(\boldsymbol{\Phi_1}\left(T_h^{(i)}\right),T_h^{(i)}\right),$$
$$T_h^*=\min\left\{\max\left\{T_h^{(i)}-\gamma\beta^j l\left[T_h^{(i)}\right],\mu_1\right\},\mu_2\right\},\gamma\beta^j\ge\varepsilon\}\cup\{0\}$$

for some fixed $\gamma\in(0,+\infty)$, $\beta\in(0,1)$, $\varepsilon\in(0,\gamma)$.

For practical implementation of the given gradient projection algorithm we would use the following flow diagram:

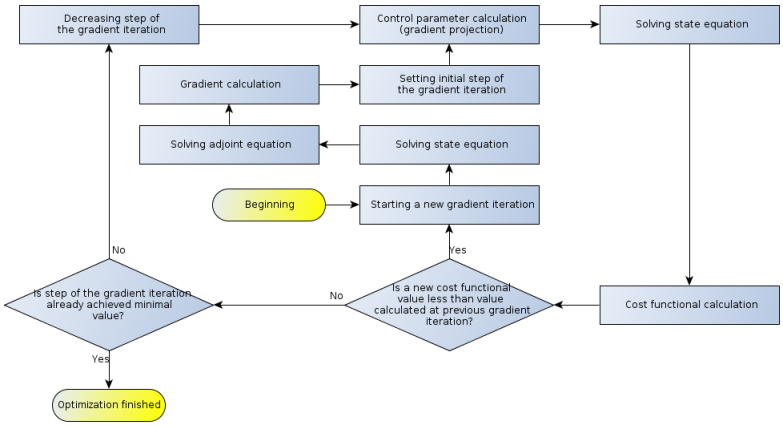

Scheme 1. Optimization (gradient projection) algorithm.

As it is easy to see from this diagram that each iteration of the proposed gradient projection algorithm includes several steps:

1. Solving of the state equation;
2. Solving of the adjoint equation and gradient calculation;
3. Using line search algorithm and repeated solving of the state equation in order to find optimal gradient iteration step;
4. Calculation of improved control parameter and transition to the next gradient iteration.

4. Methods for solving of state and adjoint equations

As it is easy to see from description of the gradient projection algorithm, then in case of the problem (8) each gradient iteration involves at least one inversion of the adjoint equation and up to $\left(\left[\log_{1/\beta}(\gamma/\varepsilon)\right]+2\right)$ inversions of the state equation. Therefore efficiency of the optimization algorithm largely depends on efficiency of inversion methods of the state and adjoint equations.

In order to choose the best method, we tried several methods for solving of the state and adjoint equations.

Now, in order to proceed further, let us rewrite the state equation (10) and the adjoint equation (13) in operator form. First of all, let us define

$$\begin{aligned}
&\boldsymbol{L_1}: V_5(\Omega_1,\Sigma_1) \to \dot{V}_5^*(\Omega_1,\Gamma_1,\Sigma_1),\\
&\boldsymbol{A_1}: V_5(\Omega_1,\Sigma_1) \to \dot{V}_5^*(\Omega_1,\Gamma_1,\Sigma_1),\\
&\boldsymbol{L_2}: W_2^1(\Omega_1,\Gamma_1) \to \left(W_2^1(\Omega_1,\Gamma_1)\right)^*,\\
&\boldsymbol{A_2}: W_2^1(\Omega_1,\Gamma_1) \to \left(W_2^1(\Omega_1,\Gamma_1)\right)^*
\end{aligned}$$

as

$$\begin{aligned}
&\langle \boldsymbol{L_1}(T_f),\eta\rangle_{\dot{V}_5(\Omega_1,\Gamma_1,\Sigma_1)} :=\\
&\qquad \int_{\Omega_1}\left(k_1(\nabla T_f\cdot\nabla\eta)+k_2\frac{\partial T_f}{\partial x_1}\eta\right)dx+\int_{\Sigma_1}k_3(T_f-T_g)\eta ds\\
&\qquad -\sigma\int_{\Sigma_1}\left[\boldsymbol{H_2}(\psi(T_h))\right]\eta ds,\\
&\langle \boldsymbol{A_1}(T_f),\eta\rangle_{\dot{V}_5(\Omega_1,\Gamma_1,\Sigma_1)} :=\\
&\qquad \sigma\int_{\Sigma_1}\left[(\boldsymbol{E}-\boldsymbol{H_1})\left(\psi(T_f)\right)\right]\eta ds,\\
&\langle \boldsymbol{L_2}(\vartheta_*),\eta\rangle_{W_2^1(\Omega_1,\Gamma_1)} :=
\end{aligned}$$

$$\int_{\Omega_1}\left(k_1(\nabla\vartheta_*\cdot\nabla\eta)-k_2\frac{\partial\vartheta_*}{\partial x_1}\eta\right)dx+\int_{\Gamma_2}k_2\vartheta_*\eta ds$$
$$+\int_{\Sigma_1}k_3\vartheta_*\eta ds+\int_{\Omega_1}2\left(T_f-T_t\right)\eta dx,$$
$$\langle \boldsymbol{A_2}(\vartheta_*),\eta\rangle_{W_2^1(\Omega_1,\Gamma_1)}:=$$
$$\sigma\int_{\Sigma_1}\psi'\left(T_f\right)[(\boldsymbol{E}-\boldsymbol{H_1})(\vartheta_*)]\eta ds.$$

Therefore, if we denote $\boldsymbol{R_1}:=\boldsymbol{L_1}+\boldsymbol{A_1}$ and $\boldsymbol{R_2}:=\boldsymbol{L_2}+\boldsymbol{A_2}$, then the equations (10), (13) can be rewritten in the following way:

$$\boldsymbol{R_1}\left(T_f\right)=0,\ \boldsymbol{R_2}(\vartheta_*)=0.$$

4.1.Virtual time method

As first variant for numerical solving of the state and adjoint equations we developed an algorithm based on transient continuation and linearization techniques.

Since the state equation of the problem (8) is elliptical boundary value problem, then, in order to obtain simple iterative algorithm for solving of this problem, we can use standard transient continuation technique (see [7]). Using this technique, at first the original elliptic boundary value problem is artificially transformed into a new parabolic problem by introducing a virtual time variable. Afterwards by discretization of this parabolic problem along the virual time variable using Euler implicit schema, we will obtain

$$\begin{cases}\frac{\boldsymbol{E}\left(T_f^{(n+1)}\right)-\boldsymbol{E}\left(T_f^{(n)}\right)}{\tau^{(n)}}=-\boldsymbol{R_1}\left(T_f^{(n+1)}\right),\\ T_f^{(0)}=T_{f0},\\ n=0,1,\ldots,\end{cases}\quad(15)$$

where $\tau^{(n)}$ is calculated using a SER (switched evolution relaxation) formula (defined later). Here T_{f0} is some initial guess, whereas $T_f^{(n)}$ is n-th approximation of T_f.

In order to obtain final form of the algorithm, let us define the following operator:

$$\boldsymbol{P_1}[\phi]\colon V_5(\Omega_1,\Sigma_1)\to\dot{V}_5^*(\Omega_1,\Gamma_1,\Sigma_1)$$

(for fixed $\phi\in V_5(\Omega_1,\Sigma_1)$) as

$$\langle \boldsymbol{P_1}[\phi](v),\eta\rangle_{\dot{V}_5(\Omega_1,\Gamma_1,\Sigma_1)}:=\sigma\int_{\Sigma_1}\varepsilon_f\psi'(\phi)v\eta ds.$$

Due to uniform monotonicity of $\boldsymbol{M_1}[\tau,\phi]:=(\boldsymbol{E}+\tau\boldsymbol{L_1}+\tau\boldsymbol{P_1}[\phi])$ (for fixed $\tau\in(0,+\infty)$, $\phi\in V_5(\Omega_1,\Sigma_1)$), there exists continuous inverse operator $\boldsymbol{M_1}[\tau,\phi]^{-1}$. Therefore, if we define $\boldsymbol{N_1}[\tau,\phi]:=\tau(\boldsymbol{P_1}[\phi]-\boldsymbol{A_1})$, then we can rewrite the first equation of (15) in an equivalent form:

$$T_f^{(n+1)}=\boldsymbol{M_1}\left[\tau^{(n)},T_f^{(n)}\right]^{-1}\left(\boldsymbol{N_1}\left[\tau^{(n)},T_f^{(n)}\right]\left(T_f^{(n+1)}\right)+\boldsymbol{E}\left(T_f^{(n)}\right)\right).$$

By taking this into account and by applying simple iteration method for solving of this equation, we will obtain:

$$\begin{cases}T_f^{(n+1,k+1)}=\boldsymbol{M_1}\left[\tau^{(n)},T_f^{(n,k(n))}\right]^{-1}\left(\boldsymbol{N_1}\left[\tau^{(n)},T_f^{(n,k(n))}\right]\left(T_f^{(n+1,k)}\right)+\boldsymbol{E}\left(T_f^{(n,k(n))}\right)\right),\\ T_f^{(0,0)}=T_{f0},\\ n=0,1,\ldots,\ \ k=0,1,\ldots,k(n)-1,\ \ k(0)=0,\end{cases}\quad(16)$$

where $T_f^{(n,k(n))}$ is n-th approximation of T_f, but $\tau^{(n)}$ we calculate using the following formula:

$$\tau^{(n)} = \min\left\{\tau_1 \frac{\left\|\boldsymbol{R_1}\left(T_f^{(0,k(0))}\right)\right\|_{\dot{V}_5^*(\Omega_1,\Gamma_1,\Sigma_1)}}{\left\|\boldsymbol{R_1}\left(T_f^{(n,k(n))}\right)\right\|_{\dot{V}_5^*(\Omega_1,\Gamma_1,\Sigma_1)}}, \tau_2\right\}.$$

Here values of the parameters $\tau_1 \in (0, +\infty)$, $\tau_2 \in [\tau_1, +\infty)$ we must choose such a way to guarantee convergence of the algorithm (16).

Also for the adjoint equation (12) we can use similar technique, to obtain simple iterative algorithm for solving of this equation. In this case situation is even simpler, since iteration scheme:

$$\begin{cases} \frac{\boldsymbol{E}\left(\vartheta_*^{(n+1)}\right) - \boldsymbol{E}\left(\vartheta_*^{(n)}\right)}{\tau^{(n)}} = -\boldsymbol{R_2}\left(\vartheta_*^{(n+1)}\right), \\ \vartheta_*^{(0)} = \vartheta_{*0}, \\ n = 0,1, \ldots, \end{cases} \quad (17)$$

is linear with respect unknown variable $\vartheta_*^{(n+1)}$ and therefore we do not need to supplement another level of iterations in (17) in order to solve the first equation of this scheme. Therefore, if we define $\boldsymbol{M_2}[\tau] := (\boldsymbol{E} + \tau \boldsymbol{L_2})$ (for fixed $\tau \in (0, +\infty)$), then due to uniform monotonicity of this operator, there exists continuous inverse operator $\boldsymbol{M_2}[\tau]^{-1}$. But then, if we define $\boldsymbol{N_2}[\tau, \phi] := -\tau \boldsymbol{A_1}$, then we can rewrite the first equation of (17) in an equivalent form:

$$\vartheta_*^{(n+1)} = \boldsymbol{M_2}\left[\tau^{(n)}\right]^{-1}\left(\boldsymbol{N_2}\left[\tau^{(n)}\right]\left(\vartheta_*^{(n+1)}\right) + \boldsymbol{E}\left(\vartheta_*^{(n)}\right)\right).$$

If we take this into account, then we will obtain:

$$\begin{cases} \vartheta_*^{(n+1)} = \boldsymbol{M_2}\left[\tau^{(n)}\right]^{-1}\left(\boldsymbol{N_2}\left[\tau^{(n)}\right]\left(\vartheta_*^{(n+1)}\right) + \boldsymbol{E}\left(\vartheta_*^{(n)}\right)\right), \\ \vartheta_*^{(0)} = 0, \\ n = 0,1, \ldots, \end{cases} \quad (18)$$

where $\vartheta_*^{(n)}$ is n-th approximation of ϑ_*, but $\tau^{(n)}$ we calculate using the following formula:

$$\tau^{(n)} = \min\left\{\tau_1 \frac{\left\|\boldsymbol{R_2}\left(\vartheta_*^{(0)}\right)\right\|_{\left(W_2^1(\Omega_1,\Gamma_1)\right)^*}}{\left\|\boldsymbol{R_2}\left(\vartheta_*^{(n)}\right)\right\|_{\left(W_2^1(\Omega_1,\Gamma_1)\right)^*}}, \tau_2\right\}.$$

Here values of the parameters $\tau_1 \in (0, +\infty)$, $\tau_2 \in [\tau_1, +\infty)$ we must choose such a way to guarantee convergence of the algorithm (18).

In order to implement the iteration schemes (16), (18), we must discretize equations, which appear in these schemes, using one of the commonly used approaches – finite difference method, finite value method or finite element method. We chose finite volume method for this purpose.

Since open source library OpenFOAM is intended for solving of PDE boundary value problems for arbitrary defined 3D geometries using finite volume approach, then we chose this library as base for implementation of the iteration schemes (16), (18).

The iteration schemes (16), (18) for solving of the state and the adjoint equations we implemented according to the following flow diagrams:

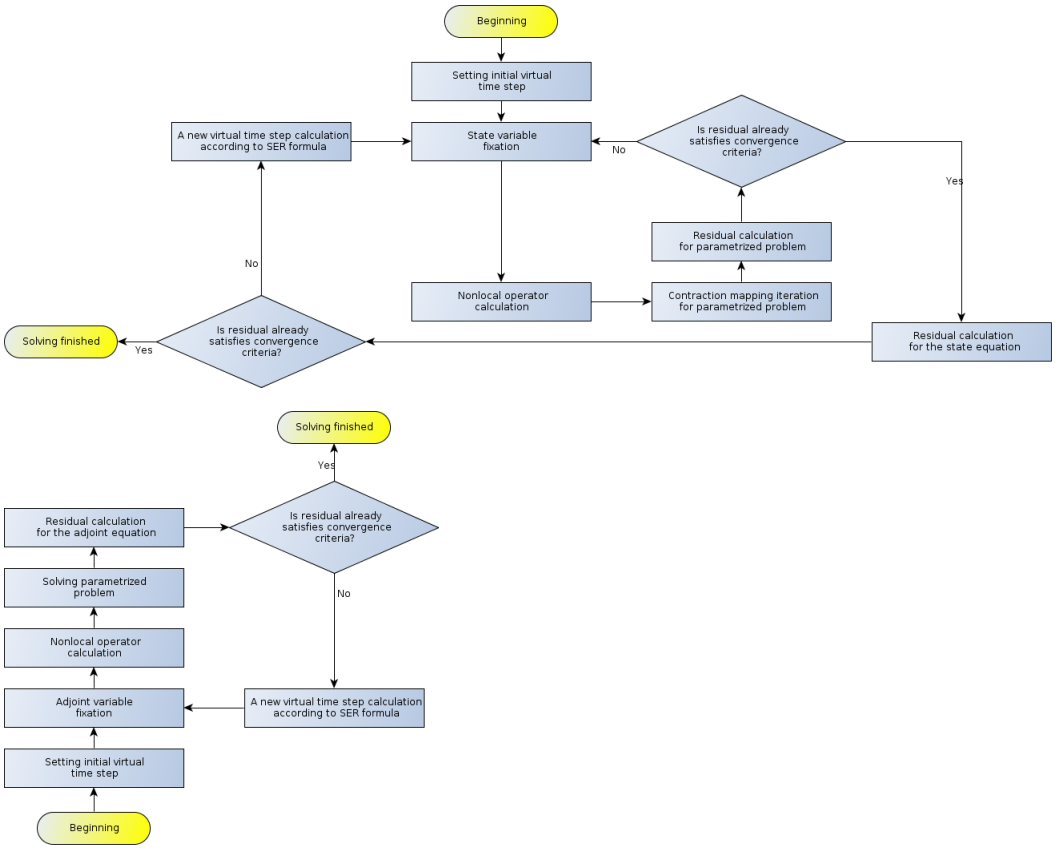

Scheme 2. Virtual time method for solving of the state and adjoint equations.

Here we must note, that, although the real implementations of (16), (18) work excelent in practice, however it is not clear yet, how to prove the following convergence result:

$$T_f^{(n,k(n))} \xrightarrow{V_5(\Omega_1,\Sigma_1)} T_f, \quad \vartheta_*^{(n)} \xrightarrow{W_2^1(\Omega_1,\Gamma_1)} \vartheta_*,$$

as $n \to +\infty$.

4.2.Contraction mapping method

As second variant for numerical solving of the state and adjoint equations we developed an algorithm based on simple iteration method for contraction mapping.

In order to obtain an algorithm for solving of the state equation of (8), let us define operators:

$$\boldsymbol{U_1}[\phi]: \dot{V}_5(\Omega_1,\Gamma_1,\Sigma_1) \to \dot{V}_5^*(\Omega_1,\Gamma_1,\Sigma_1),$$
$$\boldsymbol{T_1}: V_5(\Omega_1,\Sigma_1) \to \dot{V}_5^*(\Omega_1,\Gamma_1,\Sigma_1),$$

(for fixed $\phi \in V_5(\Omega_1,\Sigma_1)$) as

$$\langle \boldsymbol{U_1}[\phi](v),\eta\rangle_{\dot{V}_5(\Omega_1,\Gamma_1,\Sigma_1)} :=$$
$$\int_{\Omega_1}\left(k_1(\nabla v\cdot\nabla\eta)+k_2\frac{\partial v}{\partial x_1}\eta\right)dx+\int_{\Sigma_1}k_3 v\eta ds$$
$$+\sigma\int_{\Sigma_1}\varepsilon_f\psi'(\phi)v\eta ds,$$
$$\langle \boldsymbol{T_1}(v),\eta\rangle_{\dot{V}_5(\Omega_1,\Gamma_1,\Sigma_1)} :=$$
$$\sigma\int_{\Sigma_1}\varepsilon_f\psi(v)\eta ds.$$

Due to uniform monotonicity of $\boldsymbol{M_1} := (\boldsymbol{L_1}+\boldsymbol{T_1})$, there exists continuous inverse operator $\boldsymbol{M_1}^{-1}$. Therefore, if we define $\boldsymbol{N_1} := (\boldsymbol{A_1}-\boldsymbol{T_1})$ and take into account, that

$\boldsymbol{R_1} := (\boldsymbol{M_1} + \boldsymbol{N_1})$, then we can rewrite the original state equation in an equivalent form:

$$\boldsymbol{E}(T_f) + \boldsymbol{M_1}^{-1}\left(\boldsymbol{N_1}(T_f)\right) = 0.$$

If we take this into account, then by applying simple iteration method for this equation, we will obtain:

$$\begin{cases} T_f^{(n+1)} = -\boldsymbol{M_1}^{-1}\left(\boldsymbol{N_1}\left(T_f^{(n)}\right)\right), \\ T_f^{(0)} = T_e, \\ n = 0,1, \ldots. \end{cases} \quad (19)$$

Here T_e we choose as initial guess, whereas $T_f^{(n)}$ is n-th approximation of T_f.

Due to uniform monotonicity of $\boldsymbol{U_1}[\phi]$ (for fixed $\phi \in V_5(\Omega_1, \Sigma_1)$), there exists continuous inverse operator $\boldsymbol{U_1}[\phi]^{-1}$. Therefore, if we apply a Newton type method for calculation of $\boldsymbol{M_1}^{-1}$ in the first equation of (19), then we will obtain:

$$\begin{cases} T_f^{(n+1,k+1)} = T_f^{(n+1,k)} + \delta T_f^{(n+1,k)}, \\ \delta T_f^{(n+1,k)} = \boldsymbol{U_1}\left[T_f^{(n+1,k)}\right]^{-1}\left(\lambda_{(n+1,k)}\left(\boldsymbol{M_1}\left(T_f^{(n+1,k)}\right) + \boldsymbol{N_1}\left(T_f^{(n,k(n))}\right)\right)\right), \\ \lambda_{(n+1,k)} = \min\left\{\dfrac{\lambda}{\left\|\boldsymbol{M_1}\left(T_f^{(n+1,k)}\right) + \boldsymbol{N_1}\left(T_f^{(n,k(n))}\right)\right\|_{W_2^1(\Omega_1)}}, 1\right\}, \\ T_f^{(n,0)} = T_e, \\ n = 0,1,\ldots, \quad k = 0,1,\ldots, k(n)-1, \quad k(0) = 0, \end{cases} \quad (20)$$

where value of the parameter $\lambda \in (0, +\infty)$ we must choose sufficiently small to guarantee convergence of the algorithm (20).

Also for the adjoint equation (12) we can use similar technique, to obtain simple iterative algorithm for solving of this equation. In order to do this, let us define the following operator:

$$\boldsymbol{T_2}: W_2^1(\Omega_1, \Gamma_1) \to \left(W_2^1(\Omega_1, \Gamma_1)\right)^*$$

as

$$\langle \boldsymbol{T_2}(v), \eta \rangle_{W_2^1(\Omega_1, \Gamma_1)} := \sigma \int_{\Sigma_1} \psi'(T_f) v \eta ds.$$

Due to uniform monotonicity of $\boldsymbol{M_2} := (\boldsymbol{L_2} + \boldsymbol{T_2})$, there exists continuous inverse operator $\boldsymbol{M_2}^{-1}$. Therefore, if we define $\boldsymbol{N_2} := (\boldsymbol{A_2} - \boldsymbol{T_2})$ and take into account, that $\boldsymbol{R_2} := (\boldsymbol{M_2} + \boldsymbol{N_2})$, then we can rewrite the original adjoint equation in an equivalent form:

$$\boldsymbol{E}(\vartheta_*) + \boldsymbol{M_2}^{-1}\left(\boldsymbol{N_2}(\vartheta_*)\right) = 0.$$

If we take this into account, then by applying simple iteration method for this equation, we will obtain:

$$\begin{cases} \vartheta_*^{(n+1)} = -\boldsymbol{M_2}^{-1}\left(\boldsymbol{N_2}\left(\vartheta_*^{(n)}\right)\right), \\ \vartheta_*^{(0)} = 0, \\ n = 0,1, \ldots. \end{cases} \quad (21)$$

Here $\vartheta_*^{(n)}$ is n-th approximation of ϑ_*.

In order to implement the iteration schemes (20), (21), we must discretize equations, which appear in these schemes. Also in this case we used finite volume method for discretization.

The iteration schemes (20), (21) for solving of the state and the adjoint equations we implemented according to the following flow diagrams:

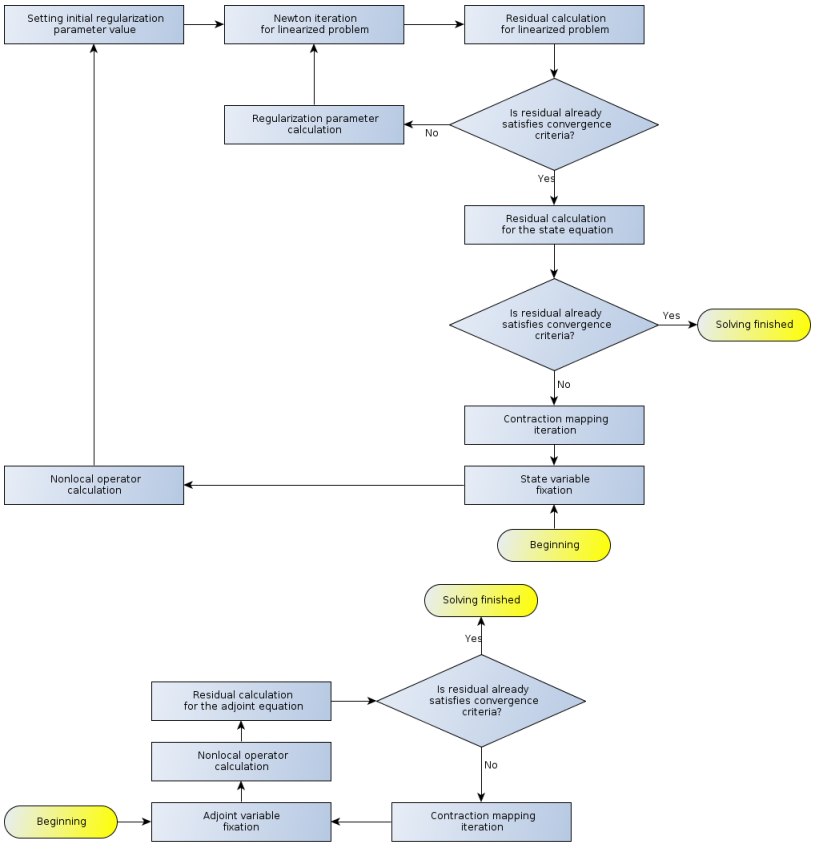

Scheme 3. Contraction mapping method for solving of the state and adjoint equations.

As it turns out, for the iteration schemes (20), (21) the following convergence result holds:

$$T_f^{(n,k(n))} \xrightarrow{V_5(\Omega_1,\Sigma_1)} T_f, \quad \vartheta_*^{(n)} \xrightarrow{W_2^1(\Omega_1,\Gamma_1)} \vartheta_*,$$

as $n \to +\infty$. Moreover, it is possible to show, that:

Theorem 4 [Convergence of discretized solutions].

For any sequence of structured meshes $\mathcal{M}_n$ ($\mathcal{M}_n$ is collection of pairwise disjoint rectangular cells $K, L, \ldots$, such that $\overline{\Omega}_1 = \bigcup_{K\in\mathcal{M}_n} \overline{K}$), where mesh size goes to 0, when $n \to +\infty$, for solutions $\tilde{T}_f^{(n,k(n))} \in L(\mathcal{M}_n)$, $\tilde{\vartheta}_*^{(n)} \in L(\mathcal{M}_n)$ ($L(\mathcal{M}_n) := \{v \in L_2(\Omega_1) : v = \sum_{K\in\mathcal{M}_n} \chi_K u_K\}$) of the discretized iteration schemes (20), (21) the following convergence result holds:

$$\tilde{T}_f^{(n,k(n))} \xrightarrow{L_2(\Omega_1)} T_f, \quad \tilde{\vartheta}_*^{(n)} \xrightarrow{L_2(\Omega_1)} \vartheta_*,$$
$$\tilde{T}_f^{(n,k(n))} \xrightarrow{L_2(\Sigma_1)} T_f, \quad \tilde{\vartheta}_*^{(n)} \xrightarrow{L_2(\Sigma_1)} \vartheta_*,$$

as $n \to +\infty$.

5. Methods for calculating of nanlocal operators

As it is easy to see, that every calculation of approximate solutions using the iteration schemes (20), (21) involves frequent calculation of values of the nonlocal operators $\boldsymbol{H_1}$, $\boldsymbol{H_2}$ (see (10), (13)). In order to obtain calculation algorithms for this purpose, we

used simple iteration method for contraction mappings and combined it with finite volume method for equation discretization.

CONTRACTION MAPPING METHOD

As it was already pointed out, that values of the operators $\boldsymbol{H_1}(v_1)$, $\boldsymbol{H_{12}}(v_2)$ for given functions $v_1 \in L_{5/4}(\Sigma_1)$, $v_2 \in L_{5/4}(\Sigma_2)$ can be calculated using the following system:

$$\begin{cases} h(x) = \sigma\big(1-\varepsilon_f\big)w(x) - \varepsilon_f \int_{n_2\cdot\omega'\geq 0} I^+(x,\omega')(n_2\cdot\omega')d\omega' & \text{on } \Sigma_1, \\ (\nabla,\omega)I = 0 & \text{on } \Lambda, \\ I^-(x,\omega) = \frac{\epsilon\sigma w}{\pi} + \frac{(1-\epsilon)}{\pi}\int_{n_2\cdot\omega'\geq 0} I^+(x,\omega')(n_2\cdot\omega')d\omega' & \text{on } \Lambda^-, \end{cases} \quad (22)$$

where

$$\boldsymbol{H_1}(v_1) := h(x) \quad \text{on } \Sigma_1, \text{if} \quad w(x) := \begin{cases} v_1(x) & \text{on } \Sigma_1, \\ 0 & \text{on } \Sigma_{2,} \\ 0 & \text{on } \Sigma_3 \end{cases} \quad (23)$$

and

$$\boldsymbol{H_2}(v_2) := h(x) \quad \text{on } \Sigma_1, \text{if} \quad w(x) := \begin{cases} 0 & \text{on } \Sigma_1, \\ v_2(x) & \text{on } \Sigma_{2,} \\ 0 & \text{on } \Sigma_3. \end{cases} \quad (24)$$

If we are using the simple iteration method for contraction mapping to solve this system, then we will get:

$$\begin{cases} h^{(n+1)}(x) = \sigma\big(1-\varepsilon_f\big)w(x) - \varepsilon_f \int_{n_2\cdot\omega'\geq 0} I^{+(n+1)}(x,\omega')(n_2\cdot\omega')d\omega' & \text{on } \Sigma_1, \\ (\nabla,\omega)I^{(n+1)} = 0 & \text{on } \Lambda, \\ I^{-(n+1)}(x,\omega) = \frac{\epsilon\sigma w}{\pi} + \frac{(1-\epsilon)}{\pi}\int_{n_2\cdot\omega'\geq 0} I^{+(n)}(x,\omega')(n_2\cdot\omega')d\omega' & \text{on } \Lambda^-, \\ I^{(0)} = 0, \\ n = 0,1,.... \end{cases} \quad (25)$$

It is possible to prove, that, if $v_1 \in L_\infty(\Sigma_1)$ and $\boldsymbol{H_1}(v_1)$ is calculated according to the formulas (23), (25), then:

$$h^{(n)} \xrightarrow{L_2(\Sigma_1)} \boldsymbol{H_1}(v_1),$$

as $n \to +\infty$. Moreover, it is possible to show, that:

Theorem 5 [Convergence of discretized solutions].

For any sequence of structured meshes $\mathcal{M}_n$ ($\overline{\Lambda} = \bigcup_{K\in\mathcal{M}_n} \overline{K}$), where mesh size goes to 0, when $n \to +\infty$, for solutions $\tilde{h}^{(n)} \in L(\mathcal{M}_n)$ ($L(\mathcal{M}_n) := \{v \in L_2(\Sigma_1) : v = \mathrm{tr}_{\Sigma_1}\big(\sum_{K\in\mathcal{M}_n} \chi_K u_K\big)\}$) of the discretized iteration scheme (25) the following convergence result holds:

$$\tilde{h}^{(n)} \xrightarrow{L_2(\Sigma_1)} \boldsymbol{H_1}(v_1),$$

as $n \to +\infty$.

Also, if $v_2 \in L_\infty(\Sigma_2)$ and $\boldsymbol{H_2}(v_2)$ is calculated according to the formulas (24), (25), then:

$$h^{(n)} \xrightarrow{L_2(\Sigma_1)} \boldsymbol{H_2}(v_2),$$

as $n \to +\infty$. Moreover, it is possible to show, that:

Theorem 6 [Convergence of discretized solutions].

For any sequence of structured meshes $\mathcal{M}_n$ *(*$\overline{\Lambda} = \bigcup_{K\in\mathcal{M}_n} \overline{K}$*), where mesh size goes to 0, when* $n \to +\infty$*, for solutions* $\tilde{h}^{(n)} \in L(\mathcal{M}_n)$ *(*$L(\mathcal{M}_n) := \{v \in L_2(\Sigma_1) : v = \mathrm{tr}_{\Sigma_1}\left(\sum_{K\in\mathcal{M}_n} \chi_K u_K\right)\}$*) of the discretized iteration scheme (25) the following convergence result holds:*

$$\tilde{h}^{(n)} \xrightarrow{L_2(\Sigma_1)} \boldsymbol{H_2}(v_2),$$

as $n \to +\infty$.

The iteration scheme (25) for calculation calculation of values of the nonlocal operators $\boldsymbol{H_1}$, $\boldsymbol{H_2}$ we implemented according to the following flow diagram:

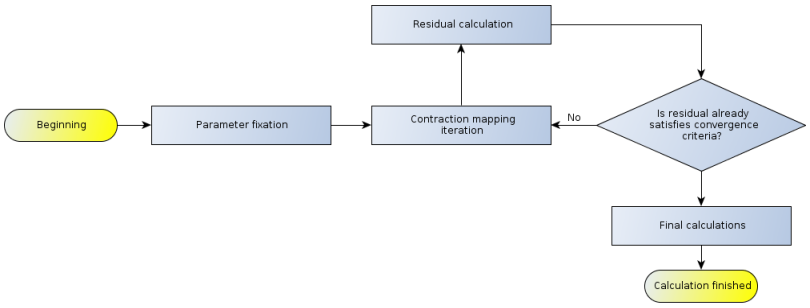

Scheme 4. Algorithm for calculation of nonlocal operators.

6. Numerical simulations

To test performance of the previously described gradient projection method we carried out some simple numerical tests. Geometry of the furnace (see Figure 2) as well as coefficient values mentioned in B1-B2 we imposed almost the same as it is described in [5]:

$$\Omega_1 := (0,3) \times (-0.55, 0.55) \times (-0.0001, 0.0001),$$
$$\Omega_2 := (0,3) \times (-0.715, 0.715) \times (-0.15, 0.2) \setminus \overline{\Omega}_1,$$
$$\Sigma_2 := \{(x_1, x_2, x_3) \in \partial\Omega_2 : 0.1 \le x_1 \le 1.3\} \setminus \partial\Omega_1.$$

Additionally we set the following bounds to the heater temperature: $\mu_1 := 303$, $\mu_2 := 1103$. To achieve quick fabric temperature increase at the entrance of the furnace and it slow decrease near the exit of the furnace, we imposed the target temperature T_t to have x_1-axis profile as shown in the Figure 3 (marked with thin dotted line).

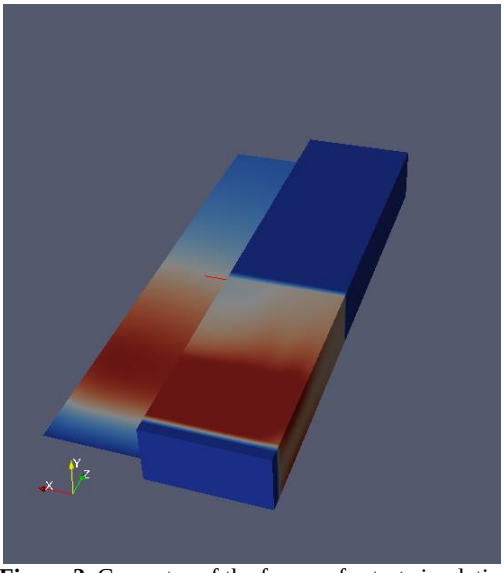

Figure 2. Geometry of the furnace for test simulation.

For discretization of (20) and (21) we used finite volume aproach (see [6], [9]). Following this approach the domain Ω_1 was split into mesh with 19440 spatial cells and $\Lambda = \Omega_2 \times S$ - into mesh with 65016 spatial cells and 32 angular cells. All numerical simulations were done using self-implemented solver based on the OpenFOAM library.

We performed several gradient descent tests starting from different initial temperature distributions on the heater. In all these cases we obtained very similar results - calculated optimal cost functional values, as well as optimal controls were nearly identical.

Constantly running many test simulations, we detected main convergence properties of the gradient descent method. At the first 10 to 20 iterations of the optimization process cost functional values decrease very fast and reach nearly optimal value (controls T_h at the same time tended to reach maximal allowed value μ_2 on some significant part of Σ_2). After that phase convergence rate of the optimization process towards minimum significantly slows down, even prohibiting calculation of optimal control in some cases.

To illustrate performance of the gradient descent method, in Table 1 we summarized optimization progress for case, when initial heater temperature was imposed to be 600K.

Iteration No	**Cost functional**	**Line search steps**
1	40.1477	1
2	19.1559	1
3	12.1004	1
…	…	…
13	1.7503	1
14	1.7276	2
15	1.7254	2

Table 1. Gradient descent test for $T_{h0} = 600$.

The temperature x_1-axis profiles of fabric and heater before and after numerical optimization for this case are shown in the Figure 3 (see also Figure 4). Thick dashed

lines mark temperature profiles before optimization, whereas thick solid lines mark temperature profiles after optimization.

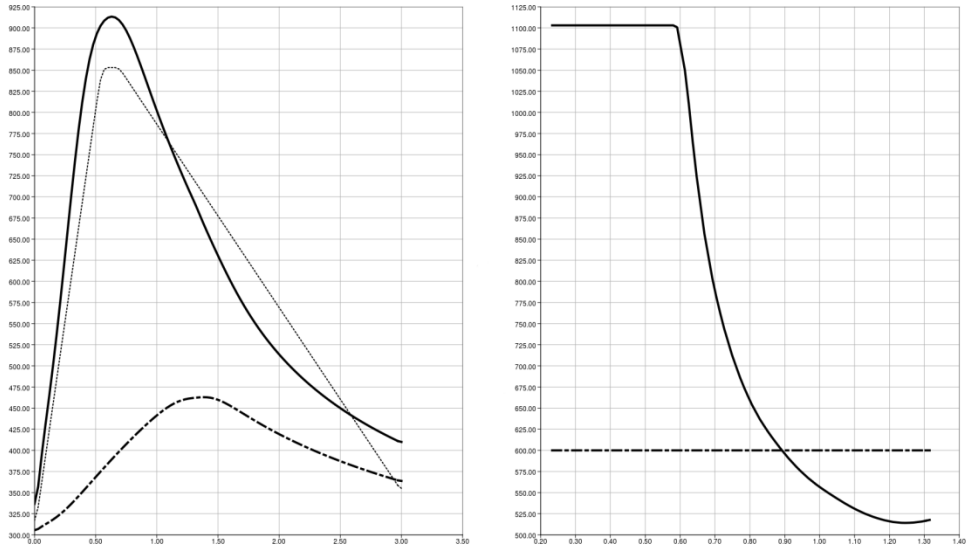

Figure 3. Temperature x_1 – axis profiles of T_t, T_f, and T_h.

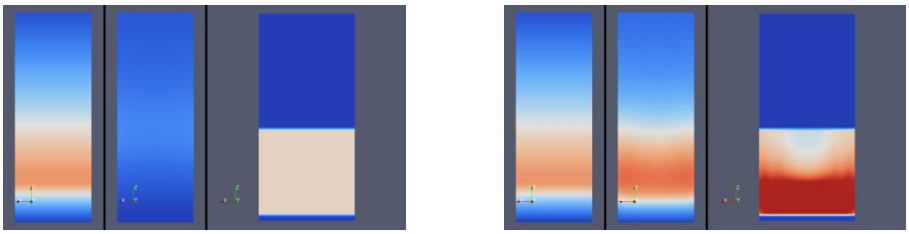

Before optimization After optimization

Figure 4. Temperature fields T_t, T_f, and T_h.

To solve the state and adjoint equations, we used the iteration schemes (20), (21). In order to illustrate performance of these schemes, in Table 2 and Table 3 (see also Figure 5) we summarized information about convergence of inner and outer iterations.

n	Residual
0	68480.47
1	13896.73
2	2928.82
3	587.30
4	114.84
5	22.15
6	4.23
7	0.80

Table 2. Convergence of outer iterations.

k	$n=1$	λ_k	$n=2$	λ_k	$n=2$	λ_k
0	68480.47	0.29	13896.73	1	2928.82	1
1	55044.67	0.36	1075.27	1	37.38	1
2	36660.21	0.54	5.43	1	0.007	1
3	18467.04	1	0.0005	1	0.0005	1
4	3249.37	1	-	-	-	-

5	274.20	1	-	-	-	-
6	2.63	1	-	-	-	-
7	0.0005	1	-	-	-	-

Table 3. Convergence of inner iterations.

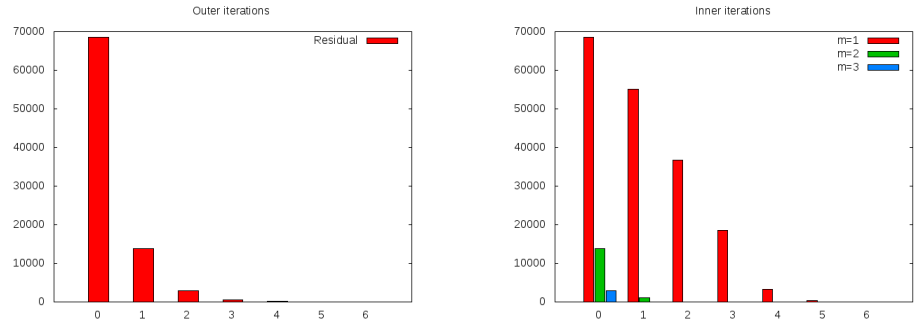

Outer iterations Inner iterations

Figure 5. Convergence of outer and inner iterations.

References

[1] **K. Birgelis and U. Raitums**. Strictly convergent algorithm for an elliptic equation with nonlocal and nonlinear boundary conditions. Mathematical Modelling and Analysis, 17(1):128–139, 2012.

[2] **V. Agoshkov**. *Boundary value problems for transport equations.* Birkhauser, Boston, 1998.

[3] **K. Birgelis**. *Optimal control in models with conductive-radiative heat transfer.* Mathematical Modelling and Analysis, 8(1):1–12, 2003.

[4] **K. Birgelis**. *Sensitivity analysis for an optimal control problem of heat transfer.* University of Latvia, Riga, 2007. (PhD Thesis).

[5] **A. Buikis and A. D. Fitt**. *A mathematical model for the heat treatment of glass fabric sheets.* IMA Journal of Mathematics Applied in Business and Industry, 10(1):55–86, 1999.

[6] **R. Eymard, T. Gallouet, and R. Herbin**. *Finite Volume Methods.* University of Wroclaw, 2010.

[7] **C. T. Kelley and D. E. Keyes**. *Convergence analysis of pseudo-transient continuation.* SIAM J. Numer. Anal., 35(2):508–523, 1998.

[8] **M. Laitinen and T. Tiihonen**. *Conductive-radiative heat transfer in grey materials.* Q. Appl. Math., 59(4):737–768, 2001.

[9] **E. M. Sparrow, W. J. Minkowycz and J. Y. Murthy**. *Handbook of numerical heat transfer.* Wiley, Hoboken, 2006.